Proceedings of the 2009 IEEE International Conference on Systems, Man, and Cybernetics
San Antonio, TX, USA - October 2009

Real-Time Upper Limb Motion Prediction from noninvasive biosignals for physical Human-Machine Interactions

Suncheol Kwon
Dept. of Mechanical Engineering
KAIST
Daejeon, Korea
norierup@kaist.ac.kr

Jung Kim
Dept. of Mechanical Engineering
KAIST
Daejeon, Korea
jungkim@kaist.ac.kr

***Abstract*— Human motion and its intention sensing from noninvasive biosignals is one of the significant issues in the field of physical human-machine interactions (pHMI). This paper presents a real-time upper limb motion prediction method using surface electromyography (sEMG) signals for pHMI. The sEMG signals from 5 channels were collected and used to predict the motion by an artificial neural network (ANN) algorithm. We designed a human-machine interaction system to verify the proposed method. Interaction experiments were performed with or without physical contact, and the effects of instances of contact were investigated. The experimental results were compared with controlled experiments using a customized goniometer, which is able to measure upper limb flexion-extension. The results showed that the proposed method was not superior to the use of direct angle measurements; however, it provides sufficient accuracy and a fast response speed for interactions. SEMG-based interactions will become more natural with further studies of human-machine combination models.**

***Keywords*—Surface electromyography, Real-time motion prediction, Physical human-machine interaction**

I. INTRODUCTION

Next generation machines are expected to interact with humans more physically and closely [1], so that these machines should be able to acquire and interpret the capabilities of human motions. If interactive machines can detect human behaviors and understand their intention, the machines can provide adequate supports. From these expectations, human motion and its intention sensing is one of the significant issues in the field of physical human-machine interaction (pHMI).

Research uses force/ torque-, tactile- and vision-sensors for human motions sensing [2-7] has flourished in the past several decades. Particularly in cooperative machine research, a machine has been shown to interpret measured force as an operator intention and then carry objects for the operator [8]. Kosuge *et al.* presented the interactive robot known as "MR helper" that used using force/torque sensors [2]. They showed that the robot could detect the force applied to an object and then lift the object with the operator. Seto *et al.* proposed a motion generation method for human-machine cooperative interaction, based on applied force sensing with the MR helper robot [9]. Takubo *et al*. developed a control method and a human-machine cooperative manipulation system using a virtual nonholonomic constraint [10]. Tsumugiwa *et al*. also suggested a variable impedance controller for human-machine cooperative tasks [11]. Their studies showed good performances and interaction feasibility; however, the sensors in their studies have some limitations. Force/torque sensors have a small degree of freedom and complicated wiring problems [12] and should be mounted on machines. Vision sensors generally have low sampling frequency, and they cannot detect occluded objects. There have been investigations of multi-sensors systems that combine different sensors to overcome these disadvantages [13]. Multi-sensors systems can provide information regarding human behaviors and intention sensing, but much work is required to synchronize and process large amounts of data [1].

As a result of exploring ways toward an alternative, neural signals are expected to be used to predict intentions. Especially, numerous studies using surface electromyography (sEMG) have been presented. SEMG signals which reflect motor commands for muscle contraction are frequently used for pHMI because of the noninvasive and simple methods associated with reading the signals [14]. SEMG signal-based machine control also can compensate the inherent delay of a machine, leading to natural interaction with a user, as the onset of the signals precedes actual human movements. Previous research presented prediction possibilities of the upper limb joint torque and related trajectories using sEMG signals [15-20]; a muscle model such as Hill's model or machine learning algorithms such as artificial neural network and fuzzy logic were used for the prediction. Although the results of these studies showed promise, most studies have been off-line analysis. Recent research has presented a real-time force/ motion prediction method of the human arm using the signals [21-25], but they investigated only remote interactions (tele-manipulation) or interactions under physical contact.

In this study, a real-time upper limb motion prediction method using sEMG signals and an ANN algorithm for cooperative interactions is described. The signals from five muscles related to the motion were acquired, and an ANN algorithm was used to model a relationship between the motion

978-1-4244-2794-9/09/$25.00 ©2009 IEEE

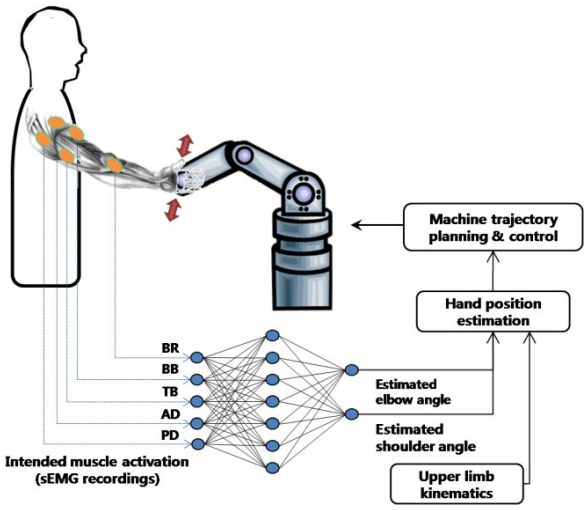

Figure 1. The overall process diagram

and the signals. An interactive machine was controlled based on predicted motion data. Additionally, sEMG-based interaction experiments were performed under contact and noncontact conditions, and the results were evaluated in comparison with controlled experiments using a customized goniometer able to measure upper limb motion with high sampling rate (1KHz) and resolution (0.09 degrees).

II. Materials and Methods

A. Overview

A diagram of the overall process is shown in Fig. 1. When a subject moves his upper limb, the subject's sEMG signals are acquired and the motion is simultaneously measured from a goniometer as a reference. An artificial neural network algorithm is used to map the relationship between the signals and measured motions. The predicted upper-limb motion data and the inverse kinematics are used to find the desired trajectory of a customized 2 degrees of freedom (DOF) manipulator.

B. SEMG signal processing

The activities of muscles were collected from five locations on the muscles related to the upper limb movements, using bipolar surface electrodes (DE-2.1, Delsys Inc., US). These locations were the *Brachioradialis* (BR), *Biceps Brachii* (BB), *Triceps Brachii* (TB), *Anterior Deltoid* (AD), and *Posterior Deltoid* (PD). The BR, BB and TB muscles are involved in forearm flexion and extension motions, and the AD/PD muscles are involved in the elevation of the upper arm. An electrode was also attached to the elbow to provide a ground reference. Fig. 2 shows the locations of the electrodes.

The signals were pre-amplified 1000 times and sampled at 1000Hz using a 16-bit A/D converting board (PCI-6034E, National Instruments, US). A third-order Butterworth IIR notch filter was used to remove unwanted 60Hz AC inference. To reject irrelevant data and noise and to emphasize the significant information in the measured signals, feature extraction of the signals is required. There are several time domain features such

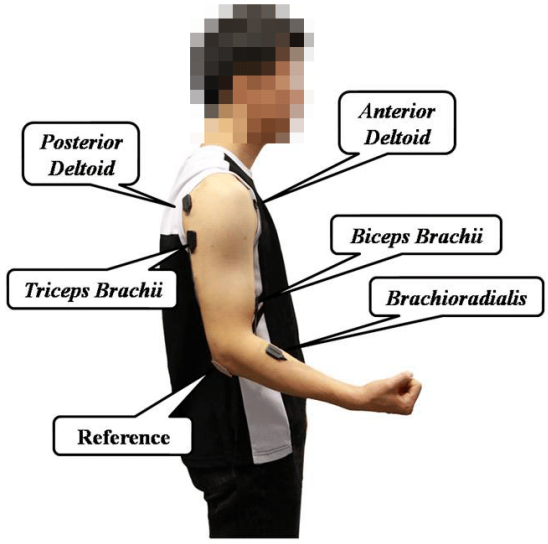

Figure 2. Surface electrodes placement

as the mean absolute value (MAV), the Willison amplitude (WAMP), and the root mean square (RMS) value [26]. Here, the RMS value of sEMG, which denotes the power of the signal [14], was extracted. As final process, the RMS value is normalized. Considering the computational load for real-time signal processing, the length of the window N was set to 200 ms. Windows were also overlapped and moved every 40ms segment step length, and the RMS of the next window was then computed. This computation process was then repeated.

C. Motion measurements

To measure the flexion-extension motion of the upper limb as reference data, a customized goniometer was used. Two incremental encoders (IRS320-1000, Sumtak Inc., Japan) that provide 4000 counts per revolution and a resolution of 0.09 degrees were mounted on the joints of the goniometer. These joints correspond to the human elbow and shoulder joint. The goniometer, like the 2DOF manipulator, can move in the 2D sagittal plane. The sprints attached to the goniometer have straps to wrap around the upper limb and ensure rigid immobilization. The linkages length and the basic position are also adjustable to fit the upper limb of a subject.

To compare the performance of the proposed method, control experiments are required. A motion capture system is usually used in controlled-experiments, but this type system has a lower resolution and sampling rate than the goniometer. Considering that the goniometer provides the best interaction performance, it was used not only to measure reference motion data but also to control the 2DOF manipulator.

D. Relationship modeling between sEMG and motion

An ANN algorithm provides a black-box model to solve complex musculoskeletal mechanics. The algorithm does not require detailed information regarding the mechanics, so that the algorithm was used to map the nonlinear relationship between the sEMG signals and the upper limb motion. The

structure of the ANN used in this study is three feed-forward layers (an input layer, a hidden layer, and an output layer). SEMG signals from five electrodes were used as inputs to the ANN, and measured motion data from the goniometer were used to train the network. The number of hidden layers was determined according to Universal Approximation Theorem [27], in which one hidden layer is considered sufficient to guarantee network convergence. It is also important that the ANN has an appropriate number of hidden neurons, as this number affects the performance of the network. After trial and error tests, the number of hidden neurons was set to twenty. A hyperbolic tangent sigmoid function and a linear function were used as neural transfer functions. The hyperbolic tangent sigmoid function calculates the activity of a hidden neuron from the total weighted sEMG inputs, as shown in (1). The linear function calculates the activity of an output neuron as prediction data from the total weighted activities of the hidden neurons, as shown in (2).

$$y_j = \frac{2}{1+e^{\{-2\times(\sum x_i w_{ji} + b_{input})\}}} - 1 \tag{1}$$

$$z_k = \sum y_j w_{kj} + b_{hidden} \tag{2}$$

where x_i is a value of the input node (sEMG feature), y_j is a value of the hidden node, z_k is a value of the output node (prediction data), w_{ij} is the connection weight between an input node and a hidden node, w_{jk} is the connection weight between a hidden node and an output node, b_{input} is the bias node at an input layer, and b_{hidden} is the bias node at a hidden layer.

For real-time interactions, changes in the weights of the network were calculated using the Levenberg-Marquardt algorithm because the algorithm provides fast convergence [18]. The algorithm converges to minimize the incidence of network error. Its formula is given as:

$$\Delta \mathbf{w} = [\mathbf{J}^T\mathbf{J} + \eta\mathbf{I}]^{-1}\mathbf{J}^T\mathbf{e} \tag{3}$$

$$\mathbf{e} = \mathbf{R} - \mathbf{z} \tag{4}$$

where $\Delta\mathbf{w}$ is a difference in the weight vectors, $\mathbf{J}$ is the Jacobian matrix that contains the first derivatives of the network errors with respect to the weight, η is a scale parameter, $\mathbf{I}$ is the identity matrix, $\mathbf{R}$ is a vector of the reference motion, $\mathbf{z}$ is a vector of the predicted motion, and $\mathbf{e}$ is a vector of network errors.

E. Experimental setup and procedure

The experimental conditions were determined using physical contact/noncontact and motion data source types as shown in Table 1. Conditions 1 and 3 indicated controlled-experiments using the goniometer. In these conditions, the interaction position was computed from measured angles between the elbow and shoulder joints. Conditions 2 and 4 were performed to evaluate the performance of the proposed

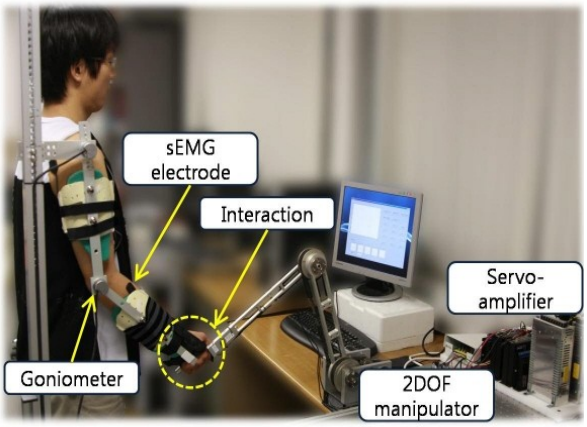

Figure 3. Experimental setup

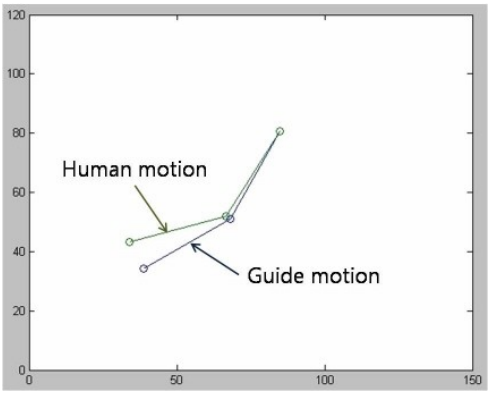

Figure 4. Motion instruction on a monitor

Figure 5. Experimental conditions according to the physical contact existence

method. In addition, experiments were performed under both physical contact and noncontact conditions. Prediction errors can be absorbed on account of the compliance of the human body under the contact condition, and there was no model pertaining to the combined effort of the operator and the machine [25]. For these reasons, experiments under the noncontact condition were performed. In order words, the subjects grasped the end-effector and moved their arm under the contact condition or move their arm without any physical contact (noncontact condition).

The overall experiment hardware setup is illustrated in Fig. 3. Prior to the experiments, six electrodes were attached as shown in Fig. 2, and the subject's arm was then tied to the goniometer using elastic straps. A subject was requested to stand and look at a computer monitor, and to move his arm according to the instructions during the experiments. During the experiments, the subject was also instructed to follow the guide motions which were expressed by blue solid segments on the monitor, and subjects' motions were represented by green solid segments, as shown in Fig. 4.

The experiments consisted of an ANN training part and test parts for each four condition. In the training part, to train the network from enough data of the upper limb motion, the sEMG signals and the arm movements of the subject which consist of the elbow and shoulder joints voluntarily flexion were collected for 170s. After the training part, during the network training for 60s, in order to prevent muscle fatigue the subject was asked to relax his arm and to avoid generating unnecessary movements apart from the flexion-extension force of the upper limb. Test time under each four condition was 60s. Five healthy and right-handed males (age 26.0 ± 2.0) volunteered for this study, and experiments were repeated five times on each subject. Each experiment was also repeated using the goniometer with a same protocol, as a control group.

III. Results

The performance of the proposed method was evaluated using three criteria: the RMS error (RMSE) and correlation coefficient (CORR) between the subject's estimated movements and the manipulator position, and the response time of the manipulator, as shown in Table 2 and Table 3. The RMSE and CORR indicate the motion prediction performance and absorption levels of prediction error. The response time also donates how quickly the manipulator reacts to subject movements.

In Table 2, the results of conditions 1 and 3 show the performance between the measured upper limb motion and the manipulator movements, and other data mean the performance of the predicted upper limb motion and the matching manipulator movements. These results show how well the manipulator was controlled using sEMG signals. When the goniometer was used to measure subject motions and to control the manipulator (Conditions 1 and 3), its performance was superior to that of the proposed method. The results were prominent because these two conditions were the control group; however, the results of the proposed method were promising.

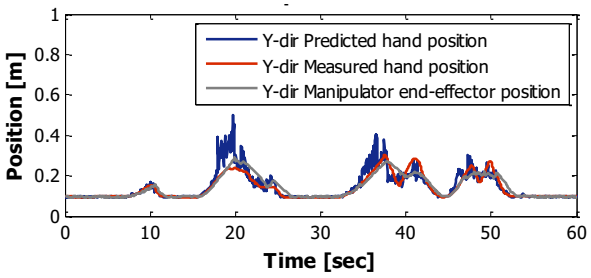

Figure 6. Estimation and manipulation results using the proposed method

TABLE I. Experimental Conditions

	Goniometer	Proposed method
Contact	Condition 1	Condition 2
Noncontact	Condition 3	Condition 4

TABLE II. Performance between the upper limb motion and the manipulator movements

Condition	RMSE [m]	CORR	Response time [ms]
1	0.009 ± 0.003	0.995 ± 0.003	80.0 ± 0.0
2	0.120 ± 0.029	0.619 ± 0.061	106.7 ± 19.5
3	0.022 ± 0.014	0.968 ± 0.029	80.0 ± 0.0
4	0.076 ± 0.023	0.801 ± 0.071	80.0 ± 26.2

TABLE III. Performance between the measured and predicted upper limb motion

Condition	RMSE[m]	CORR	Response time [ms]
1	0.210 ± 0.067	0.249 ± 0.198	-
2	0.121 ± 0.028	0.615 ± 0.073	143.3 ± 20.7
3	0.074 ± 0.020	0.849 ± 0.075	-
4	0.075 ± 0.021	0.855 ± 0.053	77.3 ± 23.7

When the signals were used under noncontact conditions, the results were better compared to contact conditions. The results under condition 1 were superior to those of condition 3. These findings suggest that the prediction error could be absorbed by the compliance of the hand and the upper limb.

Table 3 also shows the results between the measured and predicted motion of the upper limb. The results show the similarity of the predicted motion from sEMG signals and the measured motion. The performance under condition 1 was worse compared to any other condition; when the signals were used under the noncontact condition, the results were better compared to the contact condition. This implies that the motion predicted from the signals under the contact condition was not similar to the measured motion.

In addition, the response time between the manipulator movements, predicted and measured upper limb motions was investigated as shown in Table 2 and Table 3. The response time refers to the interval time between the onset of each motion rather than the phase lag between each motion. The time between the measured and predicted upper limb motion under the contact condition was constantly 80ms, as the goniometer measuring time was constant. The time under the contact condition was greater than other conditions, and the

delay under the noncontact condition was similar to the well-known electromechanical delay (EMD) of skeletal muscles (approximately 80~130ms). These results indicate that the manipulator and the upper limbs of the subjects moved almost simultaneously under the noncontact condition (2.7 ± 10.3ms). The manipulator movements, however, preceded the upper limb motion by 34.7 ± 14.1ms under the contact condition.

IV. Discussion

A. Contact and noncontact conditions

The performance of the contact condition was worse than that under the noncontact condition, as shown in Table 2 and 3. There are two possible explanations for this. The first of these involves: prediction error feedback to the subject and the training condition. Under the noncontact condition, the subject does not receive any physical feedback from the manipulator and the manipulator is controlled as in tele-manipulation. On the other hand, as shown in Fig. 7 (b), under the contact condition, the subject can receive feedback from the manipulator due to physical contact. When prediction error occurred due to the noise of the sEMG signals, inappropriate movements of the manipulator could be transferred to the subject. Additional prediction error could occur due to the abnormal sEMG signals caused by the movements of the manipulator.

However, prediction error cannot be completely transferred to the subject. Ito *et al*. showed that the wrist joint was adapted to external force, whereas the elbow and shoulder joints were independent as regards the force [28]. In other words, humans can adjust the mechanical impedance of the wrist joint and the external force caused by prediction error can be absorbed at the joint. In terms of the response time, the time between the measured and predicted arm motions was greater than the delay between the predicted arm motion and the manipulator movements as shown in Table 3. These results can be explained by the fact that the error was absorbed at the wrist during a lag.

The prediction performance under the contact condition was not good compared to the results of the noncontact condition, as sEMG signals under the contact condition had different patterns in comparison with the signals under the noncontact condition, as shown in Fig. 8, as the mass and reduction ratio of the manipulator as an external load affected muscle activation levels. In Fig. 8, for example, the maximum value of the normalized sEMG under the contact condition (0.72) was approximately twice the value under the noncontact condition (0.32); moreover, the RMS of the normalized sEMG under the contact condition during elbow movements (0.35) was also approximately twice the RMS value of the other condition (0.18). The subject moved his arm under the noncontact condition while the network training, but the trained network model was used under the contact condition. As a result, additional prediction error could be transpired. Hence, further investigation of the interaction model which takes into account the physical contact condition is required.

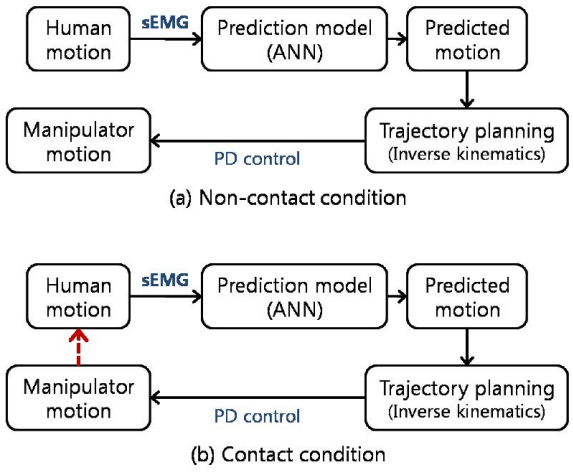

Figure 7. Prediction error feedback to human motion by physical contact

B. Feasibility of the proposed method

A key advantage of using sEMG signals for pHMI applications is that the motion prediction prior to the actual movements can compensate the delay induced by force-/tactile- and vision-sensors during the motion sensing and interactions. This point can lead to natural interaction with the subject. Under the noncontact condition, the response time between the predicted upper limb motion and the manipulator movements was similar to the time delay between the measured and predicted upper limb motion. This result demonstrates that the manipulator began to move almost simultaneously with the movements of the subject.

However, additional research is required to implement the proposed method to pHMI applications. There is no model pertaining to a combination of an operator and a machine along with the signal disturbance due to an external force. A natural human-machine interface can be achieved with the development of such a combination model.

V. Concluding Remarks

In this paper, a real-time motion prediction method using sEMG signals was proposed. We also designed a human-

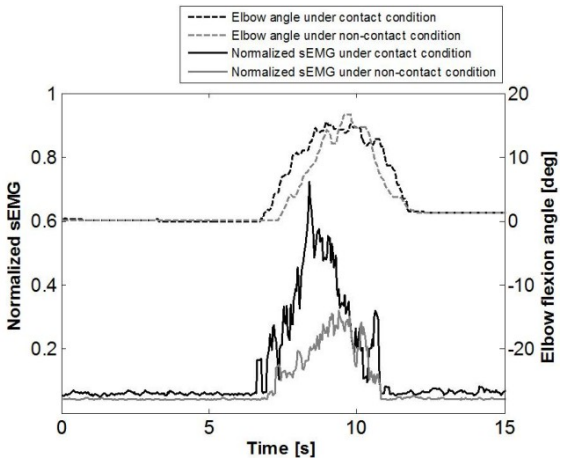

Figure 8. Different sEMG patterns according to physical contact and noncontact conditions

machine interaction system to investigate the feasibility of the proposed method for pHMI applications. Collected sEMG signals were used to predict upper limb motions by a feed-forward ANN, and the predicted motion data were then used to control a 2DOF manipulator. Interaction experiments were performed under the existence of physical contacts, and the results showed that the method can predict the motion of the upper limb successfully and that they can be used to control a manipulator. The results also demonstrated that the manipulator began to move almost simultaneously with the movements of the upper limb of the subject. Although the developed method under the noncontact condition showed feasible performance compared to previous off-line studies, the implementation of the method under the contact condition has some limitations. A system model of the sEMG disturbance that results from physical interactions is required before the proposed method can be used actually with for pHMI applications.

The next phase of this study is to increase the DOF of a predicted motion using the proposed method. Further feasibility of the method will be studied via cooperation tasks, and an interface that combines a human and a sEMG-based machine will be also modeled.

ACKNOWLEDGMENT

This work was supported partly by the Korea Institute of Science and Technology (KIST) Institutional Program and by the Korea Science and Engineering Foundation (KOSEF) grant funded by the Korea government (MOST) (No. R01-2007-000-11659 -0).

REFERENCES

[1] A. De Santis, B. Siciliano, A. De Luca, and A. Bicchi, "An atlas of physical human-robot interaction," Mechanism and Machine Theory, vol. 43, pp. 253-270, 2008.

[2] K. Kosuge, M. Sato, and N. Kazamura, "Mobile robot helper," in Proceedings of IEEE International Conference on Robotics and Automation, vol.1., pp. 583-588, 2000.

[3] A. Edsinger and C. C. Kemp, "Human-Robot Interaction for Cooperative Manipulation: Handing Objects to One Another," in Proceedings of IEEE International Symposium on Robot and Human interactive Communication, pp. 1167-1172., 2007.

[4] Z. Z. Bien, P. Kwang-Hyun, J. Jin-Woo, and D. Jun-Hyeong, "Intention reading is essential in human-friendly interfaces for the elderly and the handicapped," IEEE Transactions on Industrial Electronics, vol. 52, pp. 1500-1505, 2005.

[5] D. Kulić and E. Croft, "Pre-collision safety strategies for human-robot interaction," Autonomous Robots, vol. 22, pp. 149-164, 2007.

[6] H. Kazerooni, "Human-robot interaction via the transfer of power and information signals," IEEE Transactions on Systems, Man and Cybernetics, vol. 20, pp. 450-463, 1990.

[7] D. Erol and N. Sarkar, "Smooth Human-Robot Interaction in Robot-Assisted Rehabilitation," in Proceedings of IEEE International Conference on Rehabilitation Robotics, pp. 5-15., 2007.

[8] T. Fukuda, Y. Fujisawa, K. Kosuge, F. Arai, E. Muro, H. Hoshino, K. Miyazaki, K. Ohtsubo, and K. Uehara, "Manipulator for man-robot cooperation," in Proceedings of IEEE International Conference on Industrial Electronics, Control and Instrumentation, pp. 996-1001 vol.2., 1991.

[9] F. Seto, Y. Hirata, and K. Kosuge, "Real-time cooperating motion generation for man-machine systems and its application to medical technology," Technology and Health Care, vol. 15, pp. 121-130, 2007.

[10] T. Takubo, H. Arai, Y. Hayashibara, and K. Tanie, "Human-Robot Cooperative Manipulation Using a Virtual Nonholonomic Constraint," The International Journal of Robotics Research, vol. 21, p. 541, 2002.

[11] T. Tsumugiwa, R. Yokogawa, and K. Hara, "Variable impedance control based on estimation of human arm stiffness for human-robot cooperative calligraphic task," in Proceedings of IEEE International Conference on Robotics and Automation, vol.1., pp. 644-650, 2002.

[12] T. Tamei, S. Ishii, and T. Shibata, "Virtual Force/Tactile Sensors for Interactive Machines Using the User's Biological Signals," Advanced Robotics, vol. 22, pp. 893-911, 2008.

[13] B. Zeungnam, K. Dae-Jin, L. Hyong-Euk, P. Kwang-Hyun, S. Haiying, C. Martens, and A. Graser, "Multi sensors-based approach for intention reading with soft computing techniques," in Proceedings of IEEE International Conference on Fuzzy Systems, vol.1, pp. 596-600., 2003.

[14] C. J. De Luca, "The Use of Surface Electromyography in Biomechanics," Journal of Applied Biomechanics, vol. 13, pp. 135-163, 1997.

[15] Y. Koike and M. Kawato, "Estimation of dynamic joint torques and trajectory formation from surface electromyography signals using a neural network model," Biological Cybernetics, vol. 73, pp. 291-300, 1995.

[16] S. Morita, T. Kondo, and K. Ito, "Estimation of forearm movement from EMG signal and application to prosthetic hand control," in Proceedings of IEEE International Conference on Robotics and Automation, vol.4., pp. 3692-3697, 2001.

[17] J.-J. Luh, G.-C. Chang, C.-K. Cheng, J.-S. Lai, and T.-S. Kuo, "Isokinetic elbow joint torques estimation from surface EMG and joint kinematic data: using an artificial neural network model," Journal of Electromyography and Kinesiology, vol. 9, pp. 173-183, 1999.

[18] R. Song and K. Tong, "Using recurrent artificial neural network model to estimate voluntary elbow torque in dynamic situations," Medical and Biological Engineering and Computing, vol. 43, pp. 473-480, 2005.

[19] L. Dipietro, A. Sabatini, and P. Dario, "Artificial neural network model of the mapping between electromyographic activation and trajectory patterns in free-arm movements," Medical and Biological Engineering and Computing, vol. 41, pp. 124-132, 2003.

[20] A. T. C. Au and R. F. Kirsch, "EMG-based prediction of shoulder and elbow kinematics in able-bodied and spinal cord injured individuals," IEEE Transactions on Rehabilitation Engineering, vol. 8, pp. 471-480, 2000.

[21] J. Rosen, M. Brand, M. B. Fuchs, and M. Arcan, "A myosignal-based powered exoskeleton system," IEEE Transactions on Systems, Man and Cybernetics, vol. 31, pp. 210-222, 2001.

[22] P. K. Artemiadis and K. J. Kyriakopoulos, "EMG-based position and force control of a robot arm: Application to teleoperation and orthosis," in Proceedings of IEEE/ASME International Conference on Advanced Intelligent Mechatronics, pp. 1-6., 2007.

[23] P. K. Artemiadis and K. J. Kyriakopoulos, "Estimating arm motion and force using EMG signals: On the control of exoskeletons," in Proceedings of IEEE/RSJ International Conference on Intelligent Robots and Systems, pp. 279-284., 2008.

[24] E. E. Cavallaro, J. Rosen, J. C. Perry, and S. Burns, "Real-Time Myoprocessors for a Neural Controlled Powered Exoskeleton Arm," IEEE Transactions on Biomedical Engineering, vol. 53, pp. 2387-2396, 2006.

[25] C. Fleischer and G. Hommel, "A Human--Exoskeleton Interface Utilizing Electromyography," IEEE Transactions on Robotics, vol. 24, pp. 872-882, 2008.

[26] M. Zecca, S. Micera, M. C. Carrozza, and P. Dario, "Control of Multifunctional Prosthetic Hands by Processing the Electromyographic Signal," CRITICAL REVIEWS IN BIOMEDICAL ENGINEERING, vol. 30, pp. 459-485, 2002.

[27] S. Haykin, "Neural Networks: A Comprehensive Foundation," Printice Hall, New Jersey, USA, vol. 2., 1999.

[28] K. Ito, K. Kawakami, J. Izawa, and T. Kondo, "Upper limb impedance adjustment mechanism for dynamic environments," in Proceedings of SICE Annual Conference, vol. 3., pp. 2660-2664, 2004